https://doi.org/10.5194/egusphere-2024-1599
Preprint. Discussion started: 17 July 2024

Changes in Aerosol/Gas-Phase Distribution Ratio of Semi-Volatile Products Affect Secondary Organic Aerosol Formation with NOx from α-Pinene Photooxidation

Shijie Liu[1,2], Xinbei Xu[1], Si Zhang[1], Rongjie Li[1], Zheng Li[1], Can Wu[1], Rui Li[1], Guiqin Zhang[2], and Gehui Wang[1,3*]

[1]Key Laboratory of Geographic Information Science of the Ministry of Education, School of Geographic Sciences, East China Normal University, Shanghai 200241, China

[2]Resources and Environment Innovation Institute, Shandong Jianzhu University, Jinan 250101, China

[3]Institute of Eco-Chongming, Cuiniao Road, Chenjia Zhen, Chongming, Shanghai 202150, China

*Correspondence to: Prof. Gehui Wang (ghwang@geo.ecnu.edu.cn)

https://doi.org/10.5194/egusphere-2024-1599
Preprint. Discussion started: 17 July 2024

Abstract

Atmospheric α-pinene is one of the most important precursors of secondary organic aerosols (SOA). The formation of α-pinene derived SOA is strongly affected by NOx. However, we still do not comprehensively understand the effects of NO_x on α-pinene derived SOA formation. Therefore, we conducted α-pinene photooxidation experiments in an atmospheric chamber at different NO_x concentrations. The yields of α-pinene SOA increased with NO_x concentration under low-NO_x conditions, but were suppressed under high-NOx conditions. The maximum SOA yields were 8.0% and 26.2% in the low- and high-volatility organic compound (VOC) experiments, respectively. We found the increased SOA yields under low-NOx conditions were related to increased consumption of α-pinene. The products of α-pinene photooxidation were mainly semi-volatile, and the change in the aerosol/gas-phase distribution ratio as the formation of α-pinene photooxidation products increased was identified as the main reason for the enhanced SOA yields with increasing NOx. The sensitivity of the SOA yield to changes in NOx and VOCs under different experimental conditions was also analyzed. This study also quantified the nitrogen-containing organic compound (NOC) concentrations. The mass fraction of NOCs in SOA increased monotonically with NOx in the α-pinene photooxidation process, and the maximum NOC mass fraction made up as much as two-fifths of the α-pinene SOA.

https://doi.org/10.5194/egusphere-2024-1599
Preprint. Discussion started: 17 July 2024

1. Introduction

Fine particulate matter ($PM_{2.5}$) is an important atmospheric pollutant. Recently, $PM_{2.5}$ has attracted attention because of its negative impacts on human health, air quality, atmospheric chemical reactions, and even climate radiation balances (Bellouin et al., 2020; Wang et al., 2016). Secondary organic aerosols (SOA), which form via the atmospheric photooxidation of volatile organic compounds (VOCs), are some of the most significant sources of $PM_{2.5}$ (Lv et al., 2022; Mcfiggans et al., 2019; Zhang et al., 2018). However, due to the diversity of SOA production processes and influencing factors, much researches are still needed for the fully understand the formation mechanisms of SOA.

NO_x, which is mainly emitted from human activities, is a key substance that facilitates photooxidation. Differences in concentrations of NO_x can lead to significant changes in photooxidation processes and further affect SOA formation (Sarrafzadeh et al., 2016; Nussbaumer et al., 2022). Organic peroxyl radicals (RO_2) are the main intermediate oxidation product when VOCs are oxidized by OH. The interaction between NO_x and RO_2 plays a key role in the SOA formation process, and nonlinear relationships between NO_x and SOA yields have been observed in a large number of experimental investigations (Xu et al., 2021; Zhao et al., 2018; Sarrafzadeh et al., 2016; Xu et al., 2014). Hydroperoxides (ROOH), which are formed from the reactions of RO_2 with HO_2 or RO_2, have low volatilities and are responsible for SOA formation. However, as the concentration of NOx increases, RO_2 reacts with NO and is rapidly converted to alkoxy radicals (RO). RO act as an intermediate and goes on to produce more high volatility compounds, which suppresses SOA formation (Sarrafzadeh et al., 2016; Atkinson, 2000). Highly oxygenated organic molecules (HOMs) formed by the autoxidation of RO_2 are also key compounds involved in SOA formation (Rissanen, 2021). HOM formation is suppressed when the NO_2 concentration increases and RO_2 + NO becomes the dominant sink of RO_2 in the photooxidation process, which also contributes to the inhibition of SOA formation as NO_x concentrations increase.

https://doi.org/10.5194/egusphere-2024-1599
Preprint. Discussion started: 17 July 2024

Clearly, the effects of NO_x on photooxidation and SOA formation are quite complicated, but they have been widely studied in controlled chamber experiments. Based on the semi-volatile partitioning theory in SOA formation, it has been established that SOA yield is a function of SOA mass concentration when other experimental conditions are held constant (Odum et al., 1996; Takeuchi et al., 2022). Furthermore, the mass concentration of formed SOA is directly related to the mass concentration of available VOC precursors. However, the SOA yield is often discussed as a constant, and the nonlinear relationships between SOA yield and initial NOx concentration reported in chamber studies do not account for the consumption of VOCs (Chen et al., 2022b; Aruffo et al., 2022; Qi et al., 2020). To control for the impact of the reacted VOC concentration on SOA yields under different NOx conditions, Sarrafzadeh et al. (2016) conducted experiments that maintained similar levels of VOC consumption. However, due to differences in OH concentrations during photooxidation, there were clear differences in the reaction times in each experiment. Under normal circumstances, when exploring the impact of NOx on SOA yield, SOA yields are normalized based on the reacted VOCs concentration, but this does not account for differences in the consumption of VOCs. This approach inevitably overlooks the impact of semi-volatile partitioning theory in SOA formation under different NOx conditions. The roles of chemical processes are often considered due to the impacts of NOx on SOA yields, but physical processes in SOA formation are equally significant and should be given more attention.

α-Pinene is one of the most abundant monoterpene VOCs in the atmosphere (Sindelarova et al., 2014; Guenther et al., 2012). Due to the high concentrations and high SOA formation potential, α-pinene is one of the most important sources of SOA in the atmosphere (Xu et al., 2015a; Zhang et al., 2018). In fact, α-pinene derived SOA is commonly utilized in atmospheric models to represent biogenic SOA (Henry et al., 2012). However, further in-depth research on the mechanisms of α-pinene SOA formation is required to improve the fundamental basis and accuracy of atmospheric models. In order to fully examine the effects of NOx on SOA formation, we used an

https://doi.org/10.5194/egusphere-2024-1599
Preprint. Discussion started: 17 July 2024

indoor chamber to investigate the yields of α-pinene derived SOA with different initial NOx concentrations. The relationships among NO_x concentration, VOCs consumption, distribution of photooxidation products, and SOA mass yield were considered. Based on the semi-volatile partitioning theory, this study aimed to better characterize the mechanisms by which NO_x affect SOA yield.

2. Experimental methods

2.1. Chamber studies

A series of α-pinene photooxidation experiments initiated by NO_x were performed in a temperature controlled photooxidation chamber. The chamber and its characterization capabilities have been described in detail in our previous studies (Liu et al., 2021a; Liu et al., 2021b). In brief, the photooxidation chamber was constructed of Teflon-FEP film (0.06 mm) and surrounded with black light lamps (GE F40BLB) as the light source for the photooxidation reaction. The black light lamps provided an effective light intensity (J_{NO2}) of 0.165 min^{-1} at full illumination. Before each experiment, the chamber was cleaned by first evacuating all air and then filling it with purified air. This filling-purging cycle was repeated 5 times between experiments to ensure the residual particulate and α-pinene concentrations were less than 5 cm^{-3} and 0.5 ppb, respectively. 5 m^3 zero air, which was supplied by a zero-air generator (111-D3N, Thermo Scientific™, USA), was introduced into the chamber for the photooxidation experiment. Analytically-pure, liquid α-pinene (Sigma-Aldrich) was injected into a Teflon tube using a micro syringe, and then the α-pinene was evaporated into gas and flushed into the chamber with zero air. NOx (Air Liquid Shanghai, 510 ppm NO_2 in N_2) were introduced directly into the chamber. After all the reactants were well mixed, photooxidation of α-pinene was initiated by turning the black light lamps on. All the experiments were conducted in dry conditions with a relative humidity of 15 ± 5 %. Both OH and O_3 were formed under black light irradiation in the presence of NOx. The detailed conditions for the α-pinene photooxidation experiments are listed in Table 1. The concentrations of α-pinene were kept as constant as possible across different

https://doi.org/10.5194/egusphere-2024-1599
Preprint. Discussion started: 17 July 2024

131 experiments to ensure the effects of NO_x were not obscured. No seed particles were
132 used in the chamber experiments.

133

134 **Table 1.** Details of the α-pinene/NO_x systems used in the photooxidation experiments.

No.	α-pinene (ppb)	Δα-pinene (ppb)	NOx (ppb)	$[VOCs]_0/[NOx]_0$	SOA mass conc.[a] ($\mu g\ m^{-3}$)	SOA yield
Exp. 1	116.2	67.3	12	9.7	26.0	6.5%
Exp. 2	117.2	96.2	25	4.7	43.8	7.7%
Exp. 3	117.8	115.3	68	1.7	54.3	8.0%
Exp. 4	119.3	117.6	150	0.8	34.6	4.9%
Exp. 5	116.9	114.9	337	0.3	15.3	2.2%
Exp. 6	115.6	112.8	600	0.2	11.4	1.7%
Exp. 7	258.3	70.7	8	32.3	20.9	5.0%
Exp. 8	251.0	168.7	26	9.7	144.0	14.5%
Exp. 9	263.4	234.0	52	4.1	370.3	26.2%
Exp. 10	250.8	245.3	113	2.2	347.6	23.7%
Exp. 11	247.8	244.2	237	1.5	253.5	17.1%
Exp. 12	260.0	256.0	369	0.7	226.4	14.6%
Exp. 14	254.2	249.9	669	0.4	175.0	11.8%

135 [a] All mass concentrations were wall-loss corrected.

136 ## 2.2. On-line instruments

137 The concentration of NO_x was constantly monitored with a $NO/NO_2/NOx$ analyzer
138 (Model 42C, Thermo Corporation, USA). The α-pinene concentration was measured
139 throughout the photooxidation process with a proton-transfer-reaction time-of-flight
140 mass spectrometer (PTR-tof-MS, Ionicon Analytik, Austria) using hydronium (H_3O^+)
141 ions. The drift tube of the PTR-tof-MS was operated at 60.0 °C (T_{drift}), 2.30 mbar (P_{drift}),
142 and 600V (U_{drift}). Three ions which are commonly observed in ambient air, i.e., H_3O^+
143 (21.0226 *m/z*), NO^+ (29.9980 *m/z*), and $C_3H_6O^+$ (59.0497 *m/z*), were used for PTR-tof-
144 MS mass calibration.

145 The formation and chemical characteristics of bulk SOA were measured with a
146 high-resolution time-of-flight aerosol mass spectrometer (HR-tof-AMS, Aerodyne
147 Research Inc., USA). During which, the AMS was only operated in the V-mode in order
148 to avoid W-mode data too noisy to analyze. The ionization efficiency (IE) of the AMS
149 was calibrated via monodisperse with dried ammonium nitrate (AN) aerosols (300 nm).

https://doi.org/10.5194/egusphere-2024-1599
Preprint. Discussion started: 17 July 2024

The SOA mass concentrations obtained from AMS measurements were compared and corrected through a scanning mobility particle sizer. For SOA mass concentration calculations, the relative ionization efficiencies (RIE) of 1.4 and 1.1 were applied for organic compounds and nitrate, respectively (Middlebrook et al., 2012). The AMS data were analyzed based on the standard applications of SQUIRREL 1.51H and PIKA 1.10H in Igor Pro (WaveMetrics, Inc., USA). NO_2^+(m/z = 46)/NO^+(m/z = 30) was used to differentiate inorganic and organic nitrate in the AMS measurements (Xu et al., 2015b; Kiendler-Scharr et al., 2016; Ng et al., 2017).

3. Result and discussion

3.1 Effect of NOx on α-pinene SOA formation

The relationship between SOA yields and NO_x is shown in Fig. 1. Here, SOA yield was calculated as the SOA mass concentration divided by the reacted VOCs. Clearly, the SOA yield increased rapidly at first, reached a maximum and then decreased gradually with increasing initial NO_x concentration under both high- and low-VOC conditions. In this study, we defend the positive correlation between SOA yield and NOx as low-NOx conditions, and a negative correlation of them as high-NOx conditions. In the low- and high-VOC experiments, the maximum SOA yields were 8.0% and 26.2% respectively. Since the change trend in SOA yield with NO_x was not affected by initial VOC concentration, the effect of NO_x on SOA formation is discussed in this section using the data from the low-VOCs experiments. The concentration of VOCs in the chamber is generally higher than that in the real atmospheric environment. Lower VOC concentrations would be closer to their levels in the actual atmosphere, which would make experimental results more representative of the real atmospheric environment.

https://doi.org/10.5194/egusphere-2024-1599
Preprint. Discussion started: 17 July 2024

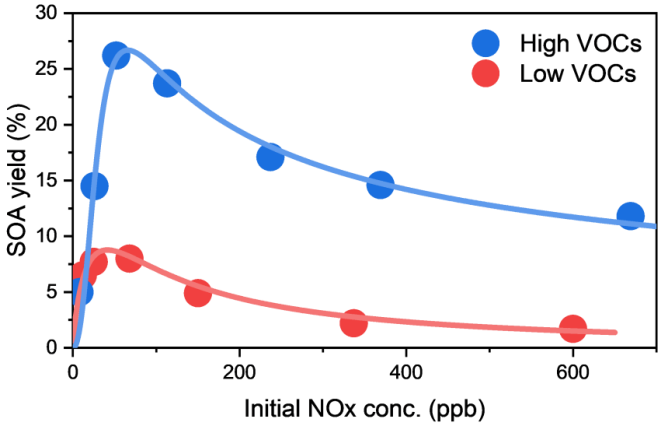

Figure 1. SOA yield from α-pinene photooxidation with different initial NO_x concentrations under two levels of VOCs.

Like our study, similar relationships between SOA yields and initial NO_x concentrations have been widely observed in previous studies (Aruffo et al., 2022; Liu et al., 2019b; Zhao et al., 2018; Lane et al., 2008; Ng et al., 2007; Kroll et al., 2006). RO_2 was the main intermediate in the photooxidation of VOCs and the concentration and fate of RO_2 depended on the NO_x concentrations. RO_2 mainly reacted with NO and was rapidly converted to alkoxy radicals (RO) under high-NO_x conditions. RO intermediates produce more high-volatility compounds than hydroperoxides (ROOH), which form through the reaction of RO_2 with RO_2/HO_2, and decrease SOA yields (Atkinson, 2000; Sarrafzadeh et al., 2016). Furthermore, the autooxidation of RO_2 can be inhibited through the RO_2 + NO / NO_2 reaction, and the reduction in HOMs further contributes to the decreased SOA yields under high-NO_x conditions (Yu et al., 2022; Laskin et al., 2018).

However, the mechanisms by which SOA yields increase with increasing NO_x concentrations under low-NO_x conditions remain poorly understood (Camredon et al., 2007; Kroll et al., 2006). The atmospheric oxidizing capacity (AOC), which indicates the oxidizing ability of the atmosphere, is significantly influenced by NOx (Wang et al., 2023). In this study, we assessed AOC based on the decay ratio of VOCs (AOC_t = -d

https://doi.org/10.5194/egusphere-2024-1599
Preprint. Discussion started: 17 July 2024

[VOCs]$_t$ / [VOCs]$_t$). The time-dependent consumption curves of VOC and the decay ratios of VOCs under different NOx concentrations are shown in Fig. 2. All experiments were allowed the same photooxidation time. For the low-NOx experiments, the consumption of α-pinene increased with NO_x concentration. Only when the initial NO_x concentration was higher than 68 ppb was α-pinene completely consumed by the end of the photooxidation period. The average decay ratio of VOCs increased from 4.75×10^{-3} to 4.53×10^{-2} as the initial NOx increased from 12 ppb to 150 ppb, and gradually decreased to 2.64×10^{-2} with an initial NOx of 600 ppb. Hence, the AOC in the chamber also showed a trend of first increasing and then decreasing with increasing NOx concentration. Sarrafzadeh et al. (2016) noted that the OH recycling reaction NO + HO_2 → NO_2 + OH was responsible for the NO_x-induced increase in OH concentration. Chen et al. (2022b) revealed that the increasing NOx level obviously enhanced the atmospheric oxidation ability in a NOx-sensitive (low-NOx) regime. The higher consumption of VOCs and the faster VOC oxidation rate both suggested there was a higher atmospheric oxidation ability in the reaction system (Ng et al., 2007). In addition, NOx is an important sink for OH, so the competition between NOx and VOCs for OH might have been responsible for the decreases in VOC consumption and AOC under high-NOx conditions.

Although there were similar trends in the yield of SOA and AOC as the NOx concentration increased, no correlation between SOA yield and AOC was observed in our study (Fig. S1). It has been shown that increases in AOC are essential drivers of increases in SOA mass concentration in the troposphere (Feng et al., 2019; Li et al., 2023). The higher SOA mass concentration under high AOC conditions was due to more VOCs being oxidized, rather than an increase in SOA yield. Therefore, the increased AOC was not the direct mechanism by which increasing NOx concentration influenced SOA yield.

https://doi.org/10.5194/egusphere-2024-1599
Preprint. Discussion started: 17 July 2024

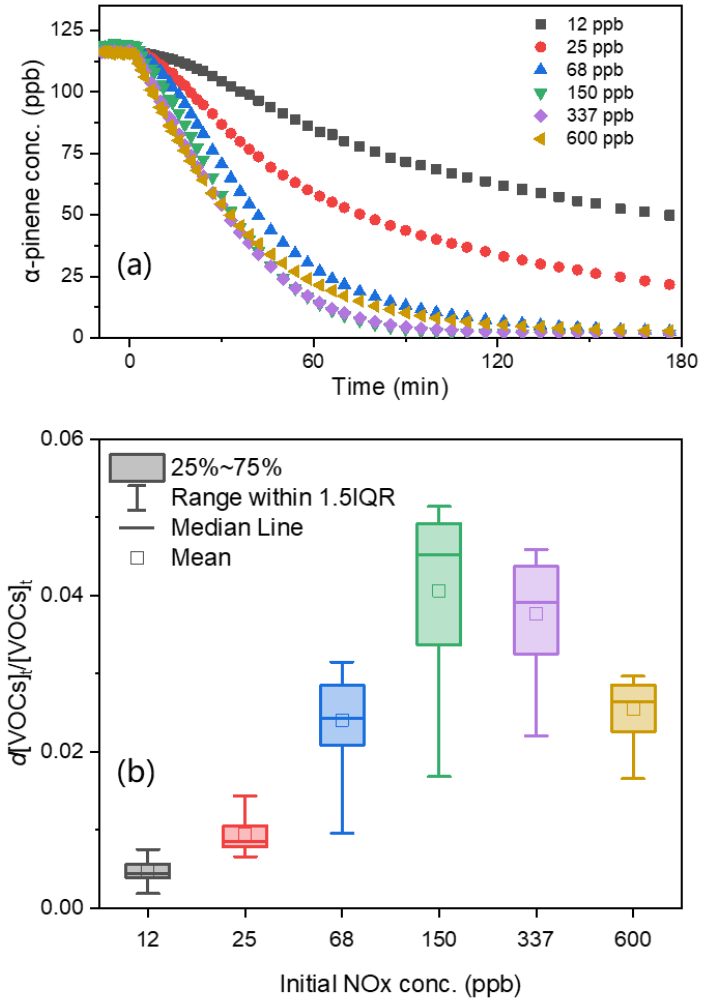

Figure 2. Changes in α-pinene concentrations over time (a) and the decay ratios of the VOCs (b) with different initial NO_x concentrations

The function of SOA yield with SOA mass concentration (M_0) was recalculated based on Odum's SOA yield model (Fig. 3). In each experiment, an increase in M_0 directly resulted in an increase in SOA yield. Notably, if the photooxidation products can be classified as low-volatility oxidation products, the SOA yield should remain constant with increasing M_0 (Krechmer et al., 2015; Ehn et al., 2014; Odum et al., 1996). However, the gas-particle distribution coefficients of semi-volatile substances are

https://doi.org/10.5194/egusphere-2024-1599
Preprint. Discussion started: 17 July 2024

directly related to their concentrations, and the distribution coefficients of semi-volatile substances into the aerosol phase are larger at higher concentrations (Akherati et al., 2019; Odum et al., 1996). Hence, the increasing distribution ratios of semi-volatile organic products between aerosol and gas phases at high M_0 were responsible for the increasing SOA yields with increasing photooxidation time (Kolesar et al., 2015; Valorso et al., 2011; Takeuchi et al., 2022).

A two-product model is an effective method for fitting the relationship between SOA yield and M_0 (Liu et al., 2019a; Odum et al., 1996). The model was calculated via equation (1), shown below:

$$Y=M_0\times\left(\frac{\alpha_1 K_{om,1}}{1+K_{om,1}M_0}+\frac{\alpha_2 K_{om,2}}{1+K_{om,2}M_0}\right) \quad (1)$$

where, M_0 is SOA mass concentration (mg m^{-3}); α_1 and α_2 are the mass-based stoichiometric coefficients of species with low-volatility and semi-volatility products, respectively; and $K_{om,1}$ and $K_{om,2}$ (m^3 μg^{-1}) are the gas-particle partitioning equilibrium constants for low-volatility and semi-volatility products, respectively. The α_1, α_2, $K_{om,1}$, and $K_{om,2}$ of α-pinene SOA formed under different initial NOx concentrations are shown in Table 2, and the simulated SOA yields with changing M_0 are shown in Fig. 3.

Table 2 Parameters of the two product model for α-derived SOA under different initial NOx concentration.

Initial NOx conc. (ppb)	α_1	$K_{om,1}$ (m^3 μg^{-1})	α_2	$K_{om,2}$ (m^3 μg^{-1})
12	0.048	0.19	0.28	0.0040
25	0.038	0.19	0.30	0.0039
68	0.028	0.19	0.32	0.0037
150	0.019	0.19	0.33	0.0031
337	0.017	0.19	0.35	0.0019
600	0.014	0.19	0.38	0.0016

It was clear that the curves of SOA yield to M_0 moved lower on the SOA yield axis in Fig. 3 with increasing NO_x concentration. According to Table 2, α_1 decreased while α_2 increased as the initial NOx concentration increased. For the experiments conducted with 12 ppb NOx, the α_1/α_2 ratio of α-pinene derived SOA was 0.17. This α_1/α_2 ratio decreased to 0.13, 0.086, 0.058, 0.049, and 0.037 as the initial NOx concentration

https://doi.org/10.5194/egusphere-2024-1599
Preprint. Discussion started: 17 July 2024

increased to 25, 68, 150, 337, and 600 ppb, respectively. Lower α_1 values indicate lower proportions of low-volatility products in the SOA, while higher α_2 values indicate higher proportions of semi-volatility products in SOA. In addition, the $K_{om,2}$ value also decreased, dropping continuously from 0.0040 to 0.0016 m^3 μg^{-1} as the initial NOx concentration increased from 12 to 600 ppb. This meant that the volatility of semi-volatility products produced through α-pinene photooxidation increased with initial NOx concentration. Overall, with increasing initial NOx concentration, the low-volatility products made up decreasing proportions (lower α_1) of the total products while semi-volatility products made up increasing proportions (higher α_2) and higher volatilities (lower $K_{om,2}$).

To determine why the volatility of SOA increase with increasing NOx, we analyzed the consumption of VOCs under different NOx conditions (Fig. 2). Due to the lower consumption rate of VOCs and low AOC, α-pinene was not completely consumed at the end of the photooxidation period under low-NOx conditions. Increased consumption of VOCs will lead to higher concentrations of photooxidation products generated in the chamber, so when the initial NOx concentration increased from 12 ppb to 25 ppb to 68 ppb, the SOA mass concentration increased from 26.0 μg m^{-3} to 43.8 μg m^{-3} to 54.3 μg m^{-3}. As mentioned above, SOA yield increased with the mass concentration of SOA. Even if the fitting curve of the two-product model gradually moved lower on the graph with increases in NOx, the SOA yield still increased from 6.5% to 8.0% when the initial NOx concentration increased from 12 ppb to 68 ppb. Hence, under low-NOx conditions, more SOA was generated due to the increased AOC and VOC consumption with increasing NOx. The enhancement of the SOA yield with increasing NOx concentrations can be attributed to the increased ratio of the aerosol/gas phase distribution resulting from higher concentrations of semi-volatile photooxidation products. Chen et al. (2022c) compared the relative content of intermediate products with different volatilities and found that the proportion of semi-volatile oxidized products in gas-phase intermediate products was lower when experiments had higher VOC consumption and SOA yields. Assuming that the proportions of different volatile

https://doi.org/10.5194/egusphere-2024-1599
Preprint. Discussion started: 17 July 2024

oxidation products remain constant, the smaller proportion of semi-volatile organic products in the gas phase suggested that a larger proportion of semi-volatile organic products was condensed into the particulate phase when more VOCs were consumed. This result also supported our conclusion that the increased aerosol/gas phase distribution ratio of semi-volatile products was the dominant driver underlying the enhanced SOA yields with increased VOC consumption under low-NOx conditions.

It should be noted that if the SOA yield is simulated based only on the two-product model, the SOA yield should increase by 34% and 51% when NOx increases from 12 ppb to 25 ppb and 68 ppb, respectively. However, in reality, the SOA yield only increased 18% and 23%, respectively (Fig. S2). The real SOA yields were not only lower than the simulated yields, but the discrepancy between the real and simulated SOA yields increased with increasing NOx concentration. As mentioned earlier, reactions between RO_2 and NOx form highly volatile oxidized compounds. Therefore, the increasing discrepancy between real and simulated SOA yields with increasing NOx concentration indicated that inhibition of SOA formation through the RO_2 + NOx reaction pathway was always occurring. This indicated that, under low-NOx conditions, the increase in SOA yield resulted from a combination of effects, the positive effect of the increased aerosol/gas phase distribution ratios of semi-volatile products and the negative effect of the RO_2 + NOx reaction.

https://doi.org/10.5194/egusphere-2024-1599
Preprint. Discussion started: 17 July 2024

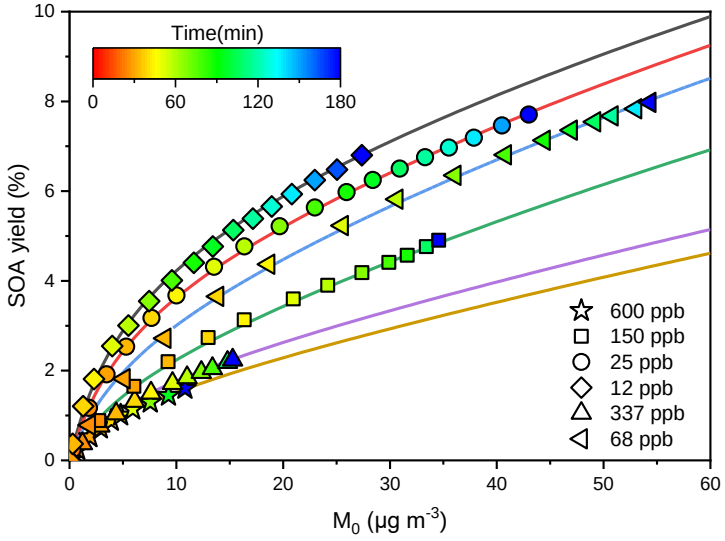

Figure 3. SOA yields as a function of organic aerosol mass concentration M_0 of α-pinene at different initial NO_x concentrations. The simulated SOA yields based on the two-product model are shown by the solid lines.

The effects of NOx on the yields and chemical properties of SOA have been well documented in previous studies (Chen et al., 2020; Eddingsaas et al., 2012; Sarrafzadeh et al., 2016; Zhao et al., 2018). However, few studies have focused on how NO_x influences VOC consumption during photooxidation, so the relationship between the concentrations of NO_x and oxidation products has not been fully elucidated. For SOA, which is mainly composed of semi-volatile oxidation products, the gas-particle distribution coefficients of semi-volatile substances are directly related to their concentrations. Therefore, SOA yield can be affected by the concentrations of semi-volatile oxidation products, and this should be taken into consideration when studying SOA formation process. Hence, future studies of photooxidation and SOA formation should pay more attention to the formation processes of semi-volatile substances.

3.2 SOA chemical composition at different NO_x concentrations

SOA chemistry must be studied at the molecular level to better understand the characteristics of SOA formation. The bulk chemical properties of SOA generated

https://doi.org/10.5194/egusphere-2024-1599
Preprint. Discussion started: 17 July 2024

under low- and high-NO_x concentrations are shown in Fig. 4.

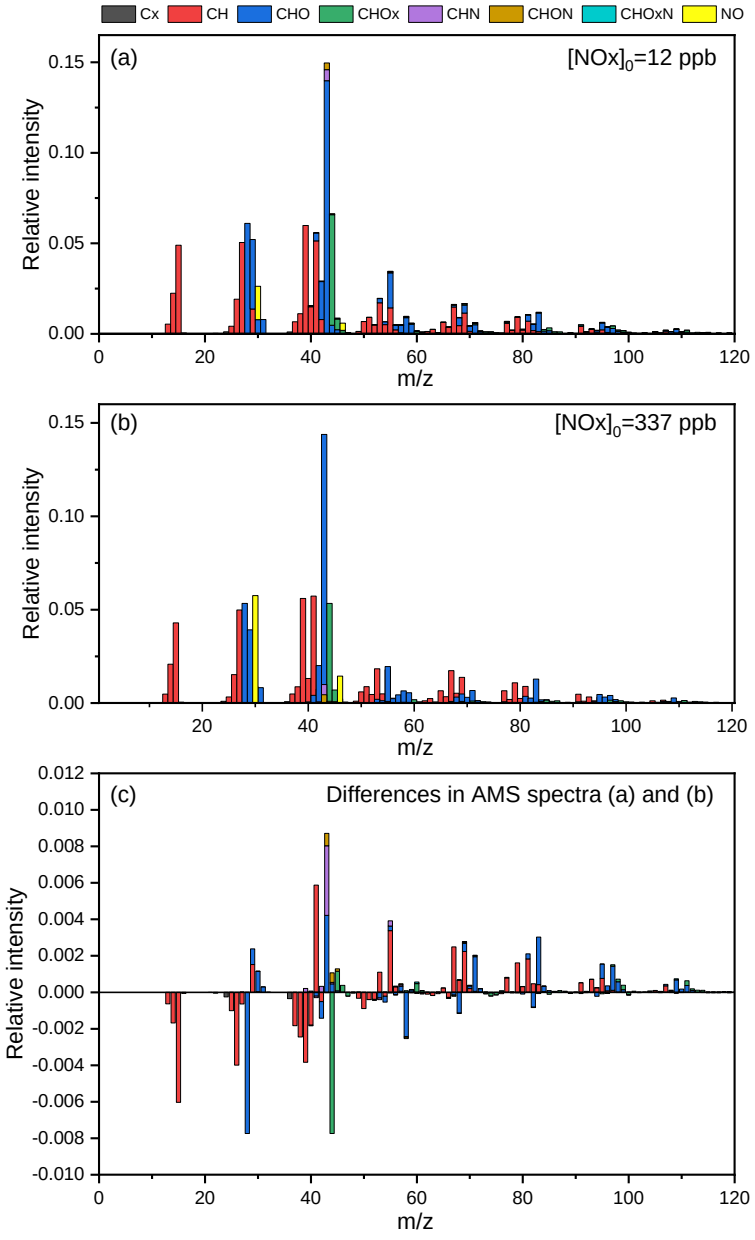

Figure 4. Typical AMS spectra of α-pinene SOA formed under low-NO_x conditions (a), high-NO_x conditions (b), and the differential spectra comparing the low- and high-NO_x conditions (c).

https://doi.org/10.5194/egusphere-2024-1599
Preprint. Discussion started: 17 July 2024

Organic fragments of $C_2H_3O^+$ (m/z = 43), which originated from the fragmentation of aldehydes and ketones, were the dominant peaks in the AMS. The strong organic AMS signal at m/z = 43 (f_{43}) indicated that the SOA oxidation level was relatively low. The intensity of the CO_2^+ (m/z = 44), representing the thermal decarboxylation of organic acid groups, was rather low, which indicated there was low carboxylic acid content in the α-pinene derived SOA. Carboxylic acid has a relatively low volatility and enters the particulate phase relatively easily, which means that the carboxylic acid produced through the photooxidation of α-pinene was likely less than that detected in the AMS. In our study, the f_{43} and f_{44} of α-pinene SOA ranged from 0.160 to 0.175 and from 0.069 to 0.074, respectively. According to the "triangle plot" of the AMS, the SOA derived from α-pinene photooxidation mainly fell in the lower area designated semi-volatile oxygenated organic aerosols (SV-OOA) (Ng et al., 2010). The AMS results provided direct evidence that semi-volatile products were the main components of α-pinene SOA formed through NO_x photooxidation. This result further supported our observations in Section 3.1, wherein the aerosol/gas-phase distribution ratio of photooxidation products increased with increasing SOA mass concentration and VOC consumption, resulting in the enhancement of SOA yield with increasing NO_x at low-NOx conditions.

The differences in the AMS spectra between low- and high-NOx conditions are compared in Fig. 4 (c). Although the inhibitory effect of the reaction between NOx and RO_2 on SOA formation was confirmed, the chemical compositions of the SOA formed under different NOx conditions showed only minor differences. Photooxidation products formed through the reaction of NO with RO_2 radicals usually have relatively high volatilities. However, the α-pinene derived SOA was mainly composed of semi-volatile photooxidation products, and these photooxidation products formed under high-NOx conditions with higher volatilities may not easily be condensed into the particulate phase, so they were mainly present in the gas phase. This means that the high volatility products formed via the RO_2 + NO reaction path under high-NOx conditions did not affect the chemical composition of SOA. Therefore, the AMS spectra

https://doi.org/10.5194/egusphere-2024-1599
Preprint. Discussion started: 17 July 2024

of the α-pinene SOA were not significantly different between low- and high-NOx conditions.

In addition to the generation of RO, the reaction of RO_2 with NO can also form N-containing compounds (NOCs). The NOC contents in SOA under different NOx conditions were calculated based on the AMS fragments of NO^+ and NO_2^+. NO^+ and NO_2^+ are characteristic fragments of NOCs, but the same NO^+ and NO_2^+ fragments can also be detected by AMS in the forms of inorganic nitrates. In order to distinguish organic nitrates from total nitrates, we used the same method as described in our previous study based on the differences in the ratios of NO^+/NO_2^+ for organic and inorganic nitrates in the AMS mass spectra (Xu et al., 2015b; Ng et al., 2017; Day et al., 2022). The concentrations of NO^+ and NO_2^+ from organic nitrates were calculated using the following equations:

$$NO_{2,org}=\frac{NO_{2,meas}\times(R_{meas}-R_{AN})}{R_{ON}-R_{AN}} \quad (4)$$

$$NO_{org}=R_{ON}\times NO_{2,org} \quad (5)$$

where R_{meas} is the NO^+/NO_2^+ ratio from the AMS results; R_{ON} and R_{AN} are the NO^+/NO_2^+ ratios for organic nitrate and ammonium nitrate, respectively; and $NO_{2,meas}$ represents the total NO_2^+ fragments obtained from the AMS data. In this study, R_{AN} was about 1.1 based on the measurements and R_{ON} was assumed to be about 10 referring to the study by Takeuchi and Ng (2019). Previous studies have shown monoterpene hydroxyl nitrate (m/z = 215), pinene keto nitrate (m/z = 229), and monoterpene dicarbonyl nitrate (m/z = 247) to be the main NOCs from α-pinene photooxidation (Chen et al., 2022a; Li et al., 2018). Here, the formation of NOCs was calculated based on organic nitrate contents and the molecular weights of NOCs.

https://doi.org/10.5194/egusphere-2024-1599
Preprint. Discussion started: 17 July 2024

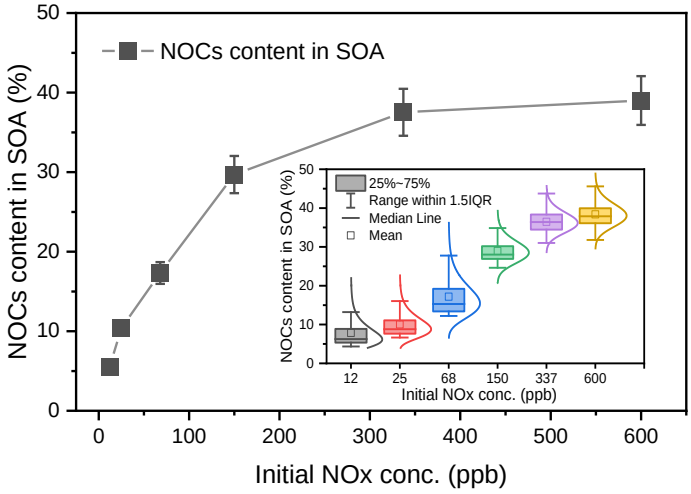

Figure 5 Content and mass concentration of NOCs under different initial NOx conditions.

The contents and mass concentrations of NOCs under different NOx levels are shown in Fig. 5. The increase in NOC contents with NOx could be divided into two stages. The first stage occurred when the initial NOx concentration increased from 12 ppb to 150 ppb. During this stage the content of NOCs in the SOA increased linearly, indicating that the NOx was the limiting factor for NOC formation in low-NOx conditions. The second stage occurred as NOx concentrations continued to rise to 600 ppb. During this stage, the growth in NOC content gradually slowed while approaching the maximum value. Based on the nonlinear fit between NOx concentration and NOC content, the maximum value of NOCs content in SOA was predicted to be about 39 ± 3.8%. This indicated that, under extremely high-NOx conditions, NOCs could account for up to two-fifths of the α-pinene SOA. These results not only showed that NOCs play a more important role in biogenic SOA formation under high-NOx conditions, but can also serve as a basis for estimating the generation of NOCs in SOA.

3.3 Effect of initial VOC concentration on SOA formation

The SOA yields with different α-pinene concentrations were also compared in this study. As shown in Fig. 1, the change trends in SOA yields with increasing NO_x

https://doi.org/10.5194/egusphere-2024-1599
Preprint. Discussion started: 17 July 2024

concentrations were similar across all experiments, including low- and high-VOC conditions. However, higher initial VOC concentrations led to increases in both maximum SOA yield and the initial NOx concentration required for the SOA yield to reach its maximum value. Under low-VOCs conditions, based on the no-linear fitting of SOA yield with initial NOx, the peak SOA yield was 8.8% when the initial NO_x concentration was 41 ppb. The maximum SOA yield increased to 26.7% under high-VOC conditions, and the concentration of NOx corresponding to the maximum SOA yield increased to 66 ppb. Under high-VOC conditions, the maximum SOA mass concentration was 370.3 μg m^{-3}. However, the maximum mass concentration of SOA formed under high-VOC conditions was only 54.3 μg m^{-3}, which was 6.8 times lower than that under high-VOCs.

Previous studies have suggested that the formation of SOA from α-pinene photooxidation is primarily limited by NOx concentration under low-NOx conditions, and variation in VOC concentrations have little effect. However, as shown in Fig. 1, the SOA yield under high-VOC conditions was consistently higher than that under low-VOC conditions. Moreover, the ratio and gap in SOA yields between high- and low-VOC conditions significantly increased with increasing NOx concentrations when NOx concentrations were lower than 60 ppb (Fig. S3). Therefore, it can be concluded that under low-NOx conditions, the formation of SOA from α-pinene photooxidation is limited by both VOCs and NOx concentration. Based on differences in VOC consumption between high- and low-VOCs conditions (Fig. S4), it appeared that, at the same NOx concentration, the consumption of VOCs was higher under high-VOC conditions and the difference in VOC consumption between high- and low-VOC conditions gradually increased with increasing NOx. According to the aerosol/gas-phase distribution ratio of semi-volatile products described in Section 3.1, higher VOC consumption can generate more semi-volatile oxidation products, which can enhance the SOA yield. The continuously increasing concentration gradient in VOC consumption between high- and low-VOC conditions indicated that the SOA yield under low-NOx conditions was also affected by the concentration of VOCs.

https://doi.org/10.5194/egusphere-2024-1599
Preprint. Discussion started: 17 July 2024

When the initial NOx concentration was higher than 100 ppb, the growth rate of the SOA yield ratio between high- and low-VOC conditions was 67.7% lower than that under low-NOx conditions. The ratio of SOA yield from high-VOC experiments was about 3–8 times higher than that from the low-VOC experiments, which surpassed the VOC ratio between different VOC conditions. This indicated that, under high-NOx conditions, SOA yield has a high sensitivity to changes in VOC concentrations, and the inhibition effect of reducing VOCs on SOA yields would be more pronounced under high-NOx conditions. It should be noted that, while the difference in VOC consumption did not change further under high-NOx conditions, the ratio of the SOA yields between high- and low-VOCs conditions continued to increase with increasing NOx concentrations. At lower VOC conditions, the RO_2 + NO pathway was more competitive, which enhanced the production of high-volatile products compared to in the higher VOC experiments. This sustained increase in the ratio of SOA yields may have been mainly due to the differences in volatilities of the oxidation products produced under high- and low-VOC conditions. Therefore, as illustrated in Fig. S3, it can be inferred that changes in VOC concentrations have a more pronounced effect on SOA yield under higher NOx conditions.

Although the trend in SOA yields with increasing NOx was similar under different VOC conditions, the change trend in AOC with increasing NOx was different (Fig. S5). First, under low-NOx conditions, the AOC under high-VOC conditions was lower than when under low-VOCs. The consumption of α-pinene was higher in the high-VOC experiments than in the low-VOC experiments and more oxidants were consumed by α-pinene under high-VOC conditions, which may have led to the inhibition of AOC. Secondly, AOC only increased with increasing NOx concentrations under high-VOC conditions. According to the fitting results in Fig. S5, under low-VOC conditions, AOC initially increased with NOx and then decreased, with an inflection point at VOCs/NOx ≈ 0.47. However, under high-VOC conditions, AOC increased with initial NOx concentration across the entire NOx gradient. Although the rate of change in AOC gradually slowed as NOx increased, no inflection point occurred in the AOC change

https://doi.org/10.5194/egusphere-2024-1599
Preprint. Discussion started: 17 July 2024

trend even when NOx reached 669 ppb, at which point VOCs/NOx decreased to 0.38. These results suggested that AOC is jointly affected by NOx and VOCs, and that VOCs/NOx is not sufficient as a direct basis for the evaluation of AOC. This demonstrated the complicated nature of accurately simulating AOC, which is an important research topic that needs to be studied further.

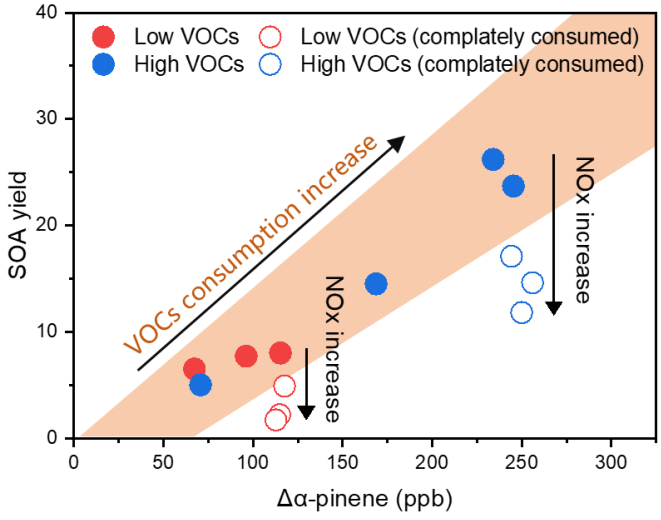

Figure 6 Relationship between consumed VOCs and SOA yields under different NOx and VOC conditions

The SOA yield trends at different AOCs are shown in Fig. S1. Based on the photooxidation experiments with different VOC concentrations, there was no clear correlation between SOA yield and AOC. This result further explains why increases in AOC are not the direct cause of increased SOA yields from α-pinene photooxidation. We further compared the consumption of VOCs with SOA yield (Fig. 6) and found a significant positive correlation between the two. This result was consistent with the study by Jiang et al. (2022) which reported that SOA yield increased with increasing consumption of VOCs, even when the OH concentration was held constant across experimental photooxidation groups. The continuous growth trend in SOA yield with increasing consumption of VOCs, which overlapped among different VOC conditions, further supported the processes discussed in Section 3.1; that is to say, changes in the aerosol/gas-phase distribution ratio for semi-volatile products with changing VOC

https://doi.org/10.5194/egusphere-2024-1599
Preprint. Discussion started: 17 July 2024

concentrations lead to increased SOA yields with increasing NOx concentration under low-NOx conditions.

However, when the NOx concentrations exceeded 68 ppb and 113 ppb under low- and high-VOC conditions, respectively, α-pinene was almost entirely consumed during the photooxidation process. This meant that, although AOC continued to increase with increasing NOx, further increases in AOC only accelerated VOC consumption time without impacting total VOC consumption or photooxidation products formation. As a result, the SOA yield did not continue to increase. In contrast, more NOx would promote the RO_2 + NO reaction, which would result in a decreasing trend in the SOA yield.

4. Atmospheric implications

NO_x is a key substrate for photooxidation in the atmosphere. Changes in NO_x concentrations can lead to significant changes in the photooxidation of VOCs and affect subsequent SOA formation. In this study, SOA yields were observed to increase sharply at first, and then decrease gradually with increasing NO_x concentration. The maximum SOA yields in the low- and high-VOC conditions were 8.0% and 26.2%, respectively. Based on the relationship between SOA yield and M_0, as well as the SOA chemical composition, semi-volatile oxidation products were the main components of α-pinene derived SOA. Under low-NO_x conditions, increasing NO_x concentration increased the consumption of VOCs during photooxidation and lead to an increase in the SOA yield. We concluded that the combination of increased distribution ratios of the semi-volatile oxidation products with increasing amounts formed was key in the promotion of SOA yield with increasing NOx. Conversely, the effect of NOx on AOC did not directly cause the increase in SOA yield. NOx can significantly increase the content of NOCs in SOA. At their highest, under extremely high-NOx concentrations, NOC contents made up as much as two-fifths of α-pinene derived SOA.

With the progression of urbanization and the changes to the natural environments surrounding urban areas, atmospheric environments of have become quite different (Xu

https://doi.org/10.5194/egusphere-2024-1599
Preprint. Discussion started: 17 July 2024

et al., 2015b; Domínguez-López et al., 2014; Shon et al., 2007; Agbo et al., 2022). Most rural areas exhibit NO_x limitation, while urban areas more often exhibit VOC limitation (Tan et al., 2018; Santos et al., 2021; Hui et al., 2018). In areas with low-NOx concentrations, the consumption of biogenic VOCs might not be significant despite there being high biogenic VOC emissions, which would limit the formation of SOA. However, if unreacted VOCs are transported to areas with high-NO_x concentrations (i.e., from rural to urban areas), or vice versa, there could be explosive increases in SOA concentrations and noticeable changes of SOA chemical compositions. Therefore, the regional transport of pollutants between urban and forested areas will significantly impact the formation of atmospheric aerosols and environmental pollution. This was supported by our study, which demonstrated how human activities can enhance SOA formation from biogenic emissions.

Finally, as a typical goal, research often works toward creating or improving models to simulate atmospheric phenomena. However, past simulations have generally underestimated SOA concentrations when compared to field observations, especially during pollution periods (Ling et al., 2022; Kelly et al., 2018). Our study noted that, under high-NOx and high-VOC conditions, SOA yield exhibited significant changes with changes in reaction conditions (Fig. S3). Under polluted conditions, the faster consumption of VOCs might lead to underestimates of VOC concentrations in the atmosphere and, subsequently, the generation of oxidation products, ultimately resulting in underestimates of SOA yields. Hence, our research provides crucial information for improving the accuracy of air quality models simulating SOA formation.

Data availability

The data used to support the conclusions in this study are available at a public data repository of Figshare via https://figshare.com/articles/dataset/NOx_photooxidation_-pinene/25200929 (S. Liu, 2024)

Author contributions

https://doi.org/10.5194/egusphere-2024-1599
Preprint. Discussion started: 17 July 2024

SL and GW designed the whole work and wrote the paper. SL did the experiment, collected the samples, conducted the sample analysis and performed the data interpretation. All authors contributed to the paper with useful scientific discussions and comments.

Competing interests

The authors declared that they have no conflict of interest.

Acknowledgements

This work was funded by the National Natural Science Foundation of China (No. 42130704, U23A2030), the China Postdoctoral Science Foundation (No. 2022T150215), and ECNU Happiness Flower Project.

Reference

Agbo, K. E., Walgraeve, C., Vandermeersch, L., Eze, J. I., Ukoha, P. O., and Van Langenhove, H.: Residential VOCs concentration levels in Nsukka, Nigeria, Atmos. Environ., 289, 10.1016/j.atmosenv.2022.119307, 2022.

Akherati, A., Cappa, C. D., Kleeman, M. J., Docherty, K. S., Jimenez, J. L., Griffith, S. M., Dusanter, S., Stevens, P. S., and Jathar, S. H.: Simulating secondary organic aerosol in a regional air quality model using the statistical oxidation model - Part 3: Assessing the influence of semi-volatile and intermediate-volatility organic compounds and NOx, Atmos. Chem. Phys., 19, 4561-4594, 10.5194/acp-19-4561-2019, 2019.

Aruffo, E., Wang, J., Ye, J., Ohno, P., Qin, Y., Stewart, M., McKinney, K., Di Carlo, P., and Martin, S. T.: Partitioning of organonitrates in the production of secondary organic aerosols from α-pinene photo-oxidation, Environ. Sci. Technol., 56, 5421-5429, 10.1021/acs.est.1c08380, 2022.

Atkinson, R.: Atmospheric chemistry of VOCs and NOx, Atmos. Environ., 34, 2063-2101, 10.1016/S1352-2310(99)00460-4, 2000.

Bellouin, N., Quaas, J., Gryspeerdt, E., Kinne, S., Stier, P., Watson-Parris, D., Boucher, O., Carslaw, K. S., Christensen, M., Daniau, A. L., Dufresne, J. L., Feingold, G., Fiedler, S., Forster, P., Gettelman, A., Haywood, J. M., Lohmann, U., Malavelle, F., Mauritsen, T., McCoy, D. T., Myhre, G., Mulmenstadt, J., Neubauer, D., Possner, A., Rugenstein, M., Sato, Y., Schulz, M., Schwartz, S. E., Sourdeval, O., Storelvmo, T., Toll, V., Winker, D., and Stevens, B.: Bounding global aerosol radiative forcing of climate change, Rev. Geophys., 58, e2019RG000660, 10.1029/2019RG000660, 2020.

Camredon, M., Aumont, B., Lee-Taylor, J., and Madronich, S.: The SOA/VOC/NOx system: an explicit model of secondary organic aerosol formation, Atmos. Chem. Phys., 7, 5599-5610, 10.5194/acp-7-5599-2007, 2007.

Chen, J., Wang, X., Zhang, J., Li, M., Li, H., Liu, Z., Bi, Y., Wu, D., Yin, X., Gu, R., Jiang, Y., Shan, Y., Zhao, Y., Xue, L., and Wang, W.: Particulate organic nitrates at Mount Tai in winter and spring: Variation characteristics and effects of mountain-valley breezes and elevated emission sources, Environ. Res., 212, 113182, 10.1016/j.envres.2022.113182, 2022a.

Chen, L. H., Bao, Z. E., Wu, X. C., Li, K. W., Han, L. X., Zhao, X. Y., Zhang, X., Wang, Z. H., Azzi, M., and Cen, K. F.: The effects of humidity and ammonia on the chemical composition of secondary aerosols from toluene/NOx photo-oxidation, Sci Total Environ, 728, ARTN 138671, 10.1016/j.scitotenv.2020.138671, 2020.

https://doi.org/10.5194/egusphere-2024-1599
Preprint. Discussion started: 17 July 2024

578 Chen, T., Zhang, P., Ma, Q., Chu, B., Liu, J., Ge, Y., and He, H.: Smog chamber study on the role of NOx
579 in SOA and O_3 formation from aromatic hydrocarbons, Environ. Sci. Technol., 56, 13654-13663,
580 10.1021/acs.est.2c04022, 2022b.

581 Chen, T. Z., Zhang, P., Chu, B. W., Ma, Q. X., Ge, Y. L., Liu, J., and He, H.: Secondary organic aerosol
582 formation from mixed volatile organic compounds: Effect of RO2 chemistry and precursor
583 concentration, NPJ Clim. Atmos. Sci., 5, 95, 10.1038/s41612-022-00321-y, 2022c.

584 Day, D. A., Campuzano-Jost, P., Nault, B. A., Palm, B. B., Hu, W., Guo, H., Wooldridge, P. J., Cohen, R.
585 C., Docherty, K. S., Huffman, J. A., de Sá, S. S., Martin, S. T., and Jimenez, J. L.: A systematic re-
586 evaluation of methods for quantification of bulk particle-phase organic nitrates using real-time
587 aerosol mass spectrometry, Atmos. Meas. Tech., 15, 459-483, 10.5194/amt-15-459-2022, 2022.

588 Domínguez-López, D., Adame, J. A., Hernández-Ceballos, M. A., Vaca, F., De la Morena, B. A., and
589 Bolívar, J. P.: Spatial and temporal variation of surface ozone, NO and NO_2 at urban, suburban, rural
590 and industrial sites in the southwest of the Iberian Peninsula, Environ. Monit. Assess., 186, 5337-
591 5351, 10.1007/s10661-014-3783-9, 2014.

592 Eddingsaas, N. C., Loza, C. L., Yee, L. D., Chan, M., Schilling, K. A., Chhabra, P. S., Seinfeld, J. H., and
593 Wennberg, P. O.: α-pinene photooxidation under controlled chemical conditions - Part 2: SOA yield
594 and composition in low- and high-NOx environments, Atmos. Chem. Phys., 12, 7413-7427,
595 10.5194/acp-12-7413-2012, 2012.

596 Ehn, M., Thornton, J. A., Kleist, E., Sipila, M., Junninen, H., Pullinen, I., Springer, M., Rubach, F.,
597 Tillmann, R., Lee, B., Lopez-Hilfiker, F., Andres, S., Acir, I. H., Rissanen, M., Jokinen, T.,
598 Schobesberger, S., Kangasluoma, J., Kontkanen, J., Nieminen, T., Kurten, T., Nielsen, L. B.,
599 Jorgensen, S., Kjaergaard, H. G., Canagaratna, M., Maso, M. D., Berndt, T., Petaja, T., Wahner, A.,
600 Kerminen, V. M., Kulmala, M., Worsnop, D. R., Wildt, J., and Mentel, T. F.: A large source of low-
601 volatility secondary organic aerosol, Nature, 506, 476-479, 10.1038/nature13032, 2014.

602 Feng, T., Zhao, S. Y., Bei, N. F., Wu, J. R., Liu, S. X., Li, X., Liu, L., Qian, Y., Yang, Q. C., Wang, Y. C.,
603 Zhou, W. J., Cao, J. J., and Li, G. H.: Secondary organic aerosol enhanced by increasing atmospheric
604 oxidizing capacity in Beijing-Tianjin-Hebei (BTH), China, Atmos. Chem. Phys., 19, 7429-7443,
605 10.5194/acp-19-7429-2019, 2019.

606 Guenther, A. B., Jiang, X., Heald, C. L., Sakulyanontvittaya, T., Duhl, T., Emmons, L. K., and Wang, X.:
607 The Model of Emissions of Gases and Aerosols from Nature version 2.1 (MEGAN2.1): an extended
608 and updated framework for modeling biogenic emissions, Geosci. Model Dev., 5, 1471-1492,
609 10.5194/gmd-5-1471-2012, 2012.

610 Henry, K. M., Lohaus, T., and Donahue, N. M.: Organic aerosol yields from α-pinene oxidation: bridging
611 the gap between first-generation yields and aging chemistry, Environ. Sci. Technol., 46, 12347-
612 12354, 10.1021/es302060y, 2012.

613 Hui, L. R., Liu, X. G., Tan, Q. W., Feng, M., An, J. L., Qu, Y., Zhang, Y. H., and Jiang, M. Q.:
614 Characteristics, source apportionment and contribution of VOCs to ozone formation in Wuhan,
615 Central China, Atmos. Environ., 192, 55-71, 10.1016/j.atmosenv.2018.08.042, 2018.

616 Jiang, X. T., Liu, D. T., Xu, L., Tsona, N. T., and Du, L.: Assessing the influence of environmental
617 conditions on secondary organic aerosol formation from a typical biomass burning compound, J.
618 Environ. Sci., 114, 136-148, 10.1016/j.jes.2021.08.016, 2022.

619 Kelly, J. M., Doherty, R. M., O'Connor, F. M., and Mann, G. W.: The impact of biogenic, anthropogenic,
620 and biomass burning volatile organic compound emissions on regional and seasonal variations in
621 secondary organic aerosol, Atmos. Chem. Phys., 18, 7393-7422, 10.5194/acp-18-7393-2018, 2018.

622 Kiendler-Scharr, A., Mensah, A. A., Friese, E., Topping, D., Nemitz, E., Prevot, A. S. H., Äijälä, M.,
623 Allan, J., Canonaco, F., Canagaratna, M., Carbone, S., Crippa, M., Dall Osto, M., Day, D. A., De
624 Carlo, P., Di Marco, C. F., Elbern, H., Eriksson, A., Freney, E., Hao, L., Herrmann, H., Hildebrandt,
625 L., Hillamo, R., Jimenez, J. L., Laaksonen, A., McFiggans, G., Mohr, C., O'Dowd, C., Otjes, R.,
626 Ovadnevaite, J., Pandis, S. N., Poulain, L., Schlag, P., Sellegri, K., Swietlicki, E., Tiitta, P.,
627 Vermeulen, A., Wahner, A., Worsnop, D., and Wu, H.-C.: Ubiquity of organic nitrates from
628 nighttime chemistry in the European submicron aerosol, Geophys. Res. Lett., 43, 7735-7744,
629 10.1002/2016GL069239, 2016.

https://doi.org/10.5194/egusphere-2024-1599
Preprint. Discussion started: 17 July 2024

Kolesar, K. R., Chen, C., Johnson, D., and Cappa, C. D.: The influences of mass loading and rapid dilution of secondary organic aerosol on particle volatility, Atmos. Chem. Phys., 15, 9327-9343, 10.5194/acp-15-9327-2015, 2015.

Krechmer, J. E., Coggon, M. M., Massoli, P., Nguyen, T. B., Crounse, J. D., Hu, W., Day, D. A., Tyndall, G. S., Henze, D. K., Rivera-Rios, J. C., Nowak, J. B., Kimmel, J. R., Mauldin, R. L., 3rd, Stark, H., Jayne, J. T., Sipila, M., Junninen, H., Clair, J. M., Zhang, X., Feiner, P. A., Zhang, L., Miller, D. O., Brune, W. H., Keutsch, F. N., Wennberg, P. O., Seinfeld, J. H., Worsnop, D. R., Jimenez, J. L., and Canagaratna, M. R.: Formation of low volatility organic compounds and secondary organic aerosol from isoprene hydroxyhydroperoxide low-NO oxidation, Environ. Sci. Technol., 49, 10330-10339, 10.1021/acs.est.5b02031, 2015.

Kroll, J. H., Ng, N. L., Murphy, S. M., Flagan, R. C., and Seinfeld, J. H.: Secondary organic aerosol formation from isoprene photooxidation, Environ. Sci. Technol., 40, 1869-1877, 10.1021/es0524301, 2006.

Lane, T. E., Donahue, N. M., and Pandis, S. N.: Effect of NOx on secondary organic aerosol concentrations, Environ. Sci. Technol., 42, 6022-6027, 10.1021/es703225a, 2008.

Laskin, J., Laskin, A., and Nizkorodov, S. A.: Mass spectrometry analysis in atmospheric chemistry, Anal. Chem., 90, 166-189, 10.1021/acs.analchem.7b04249, 2018.

Li, R., Wang, X. F., Gu, R. R., Lu, C. Y., Zhu, F. P., Xue, L. K., Xie, H. J., Du, L., Chen, J. M., and Wang, W. X.: Identification and semi-quantification of biogenic organic nitrates in ambient particulate matters by UHPLC/ESI-MS, Atmos. Environ., 176, 140-147, 10.1016/j.atmosenv.2017.12.038, 2018.

Li, Y., Han, Z. W., Song, Y., Li, J. W., Sun, Y. L., and Wang, T. T.: Impacts of the COVID-19 lockdown on atmospheric oxidizing capacity and secondary aerosol formation over the Beijing-Tianjin-Hebei region in Winter-Spring 2020, Atmos. Environ., 295, 10.1016/j.atmosenv.2022.119540, 2023.

Ling, Z., Wu, L., Wang, Y., Shao, M., Wang, X., and Huang, W.: Roles of semivolatile and intermediate-volatility organic compounds in secondary organic aerosol formation and its implication: A review, J. Environ. Sci., 114, 259-285, 10.1016/j.jes.2021.08.055, 2022.

Liu, C. G., Liu, J., Liu, Y. C., Chen, T. Z., and He, H.: Secondary organic aerosol formation from the OH-initiated oxidation of guaiacol under different experimental conditions, Atmos. Environ., 207, 30-37, 10.1016/j.atmosenv.2019.03.021, 2019a.

Liu, S. J., Jiang, X. T., Tsona, N. T., Lv, C., and Du, L.: Effects of NOx, SO_2 and RH on the SOA formation from cyclohexene photooxidation, Chemosphere, 216, 794-804, 10.1016/j.chemosphere.2018.10.180, 2019b.

Liu, S. J., Huang, D. D., Wang, Y. Q., Zhang, S., Liu, X. D., Wu, C., Du, W., and Wang, G. H.: Synergetic effects of NH_3 and NOx on the production and optical absorption of secondary organic aerosol formation from toluene photooxidation, Atmos. Chem. Phys., 21, 17759-17773, 10.5194/acp-21-17759-2021, 2021a.

Liu, S. J., Wang, Y. Q., Wang, G. H., Zhang, S., Li, D. P., Du, L., Wu, C., Du, W., and Ge, S. S.: Enhancing effect of NO_2 on the formation of light-absorbing secondary organic aerosols from toluene photooxidation, Sci Total Environ, 794, 148714, 10.1016/j.scitotenv.2021.148714, 2021b.

Lv, S., Wang, F., Wu, C., Chen, Y., Liu, S., Zhang, S., Li, D., Du, W., Zhang, F., Wang, H., Huang, C., Fu, Q., Duan, Y., and Wang, G.: Gas-to-aerosol phase partitioning of atmospheric water-soluble organic compounds at a rural site in china: An enhancing effect of NH_3 on SOA formation, Environ. Sci. Technol., 56, 3915-3924, 10.1021/acs.est.1c06855, 2022.

McFiggans, G., Mentel, T. F., Wildt, J., Pullinen, I., Kang, S., Kleist, E., Schmitt, S., Springer, M., Tillmann, R., Wu, C., Zhao, D., Hallquist, M., Faxon, C., Le Breton, M., Hallquist, A. M., Simpson, D., Bergstrom, R., Jenkin, M. E., Ehn, M., Thornton, J. A., Alfarra, M. R., Bannan, T. J., Percival, C. J., Priestley, M., Topping, D., and Kiendler-Scharr, A.: Secondary organic aerosol reduced by mixture of atmospheric vapours, Nature, 565, 587-593, 10.1038/s41586-018-0871-y, 2019.

Middlebrook, A. M., Bahreini, R., Jimenez, J. L., and Canagaratna, M. R.: Evaluation of composition-dependent collection efficiencies for the aerodyne aerosol mass spectrometer using field data,

https://doi.org/10.5194/egusphere-2024-1599
Preprint. Discussion started: 17 July 2024

Aerosol Sci. Tech., 46, 258-271, 10.1080/02786826.2011.620041, 2012.

Ng, N. L., Kroll, J. H., Chan, A. W. H., Chhabra, P. S., Flagan, R. C., and Seinfeld, J. H.: Secondary organic aerosol formation from *m*-xylene, toluene, and benzene, Atmos. Chem. Phys., 7, 3909-3922, 10.5194/acp-7-3909-2007, 2007.

Ng, N. L., Canagaratna, M. R., Zhang, Q., Jimenez, J. L., Tian, J., Ulbrich, I. M., Kroll, J. H., Docherty, K. S., Chhabra, P. S., Bahreini, R., Murphy, S. M., Seinfeld, J. H., Hildebrandt, L., Donahue, N. M., DeCarlo, P. F., Lanz, V. A., Prévôt, A. S. H., Dinar, E., Rudich, Y., and Worsnop, D. R.: Organic aerosol components observed in Northern Hemispheric datasets from Aerosol Mass Spectrometry, Atmos. Chem. Phys., 10, 4625-4641, 10.5194/acp-10-4625-2010, 2010.

Ng, N. L., Brown, S. S., Archibald, A. T., Atlas, E., Cohen, R. C., Crowley, J. N., Day, D. A., Donahue, N. M., Fry, J. L., Fuchs, H., Griffin, R. J., Guzman, M. I., Herrmann, H., Hodzic, A., Iinuma, Y., Jimenez, J. L., Kiendler-Scharr, A., Lee, B. H., Luecken, D. J., Mao, J., McLaren, R., Mutzel, A., Osthoff, H. D., Ouyang, B., Picquet-Varrault, B., Platt, U., Pye, H. O. T., Rudich, Y., Schwantes, R. H., Shiraiwa, M., Stutz, J., Thornton, J. A., Tilgner, A., Williams, B. J., and Zaveri, R. A.: Nitrate radicals and biogenic volatile organic compounds: oxidation, mechanisms, and organic aerosol, Atmos. Chem. Phys., 17, 2103-2162, 10.5194/acp-17-2103-2017, 2017.

Nussbaumer, C. M., Pozzer, A., Tadic, I., Röder, L., Obersteiner, F., Harder, H., Lelieveld, J., and Fischer, H.: Tropospheric ozone production and chemical regime analysis during the COVID-19 lockdown over Europe, Atmos. Chem. Phys., 22, 6151-6165, 10.5194/acp-22-6151-2022, 2022.

Odum, J. R., Hoffmann, T., Bowman, F., Collins, D., Flagan, R. C., and Seinfeld, J. H.: Gas/particle partitioning and secondary organic aerosol yields, Environ. Sci. Technol., 30, 2580-2585, 10.1021/es950943+, 1996.

Qi, X., Zhu, S. P., Zhu, C. Z., Hu, J., Lou, S. R., Xu, L., Dong, J. G., and Cheng, P.: Smog chamber study of the effects of NOx and NH_3 on the formation of secondary organic aerosols and optical properties from photo-oxidation of toluene, Sci Total Environ, 727, ARTN 138632, 10.1016/j.scitotenv.2020.138632, 2020.

Rissanen, M.: Anthropogenic volatile organic compound (AVOC) autoxidation as a source of highly oxygenated organic molecules (HOM), J. Phys. Chem. A, 125, 9027-9039, 10.1021/acs.jpca.1c06465, 2021.

Santos, F. M., Gómez-Losada, A., and Pires, J. C. M.: Empirical ozone isopleths at urban and suburban sites through evolutionary procedure-based models, J. Hazard. Mater., 419, ARTN 126386, 10.1016/j.jhazmat.2021.126386, 2021.

Sarrafzadeh, M., Wildt, J., Pullinen, I., Springer, M., Kleist, E., Tillmann, R., Schmitt, S. H., Wu, C., Mentel, T. F., Zhao, D., Hastie, D. R., and Kiendler-Scharr, A.: Impact of NOx and OH on secondary organic aerosol formation from β-pinene photooxidation, Atmos. Chem. Phys., 16, 11237-11248, 10.5194/acp-16-11237-2016, 2016.

Shon, Z. H., Lee, G., Song, S. K., Lee, M., Han, J., and Lee, D.: Characteristics of reactive nitrogen compounds and other relevant trace gases in the atmosphere at urban and rural areas of Korea during May-June, 2004, J Atmos. Chem., 58, 203-218, 10.1007/s10874-007-9088-4, 2007.

Sindelarova, K., Granier, C., Bouarar, I., Guenther, A., Tilmes, S., Stavrakou, T., Müller, J. F., Kuhn, U., Stefani, P., and Knorr, W.: Global data set of biogenic VOC emissions calculated by the MEGAN model over the last 30 years, Atmos. Chem. Phys., 14, 9317-9341, 10.5194/acp-14-9317-2014, 2014.

Takeuchi, M. and Ng, N. L.: Chemical composition and hydrolysis of organic nitrate aerosol formed from hydroxyl and nitrate radical oxidation of α-pinene and β-pinene, Atmos. Chem. Phys., 19, 12749-12766, 10.5194/acp-19-12749-2019, 2019.

Takeuchi, M., Berkemeier, T., Eris, G., and Ng, N. L.: Non-linear effects of secondary organic aerosol formation and properties in multi-precursor systems, Nat. Commun., 13, 10.1038/s41467-022-35546-1, 2022.

Tan, Z. F., Lu, K. D., Dong, H. B., Hu, M., Li, X., Liu, Y. H., Lu, S. H., Shao, M., Su, R., Wang, H. C., Wu, Y. S., Wahner, A., and Zhang, Y. H.: Explicit diagnosis of the local ozone production rate and the ozone-NOx-VOC sensitivities, Sci. Bull., 63, 1067-1076, 10.1016/j.scib.2018.07.001, 2018.

https://doi.org/10.5194/egusphere-2024-1599
Preprint. Discussion started: 17 July 2024

Valorso, R., Aumont, B., Camredon, M., Raventos-Duran, T., Mouchel-Vallon, C., Ng, N. L., Seinfeld, J. H., Lee-Taylor, J., and Madronich, S.: Explicit modelling of SOA formation from α-pinene photooxidation: sensitivity to vapour pressure estimation, Atmos. Chem. Phys., 11, 6895-6910, 10.5194/acp-11-6895-2011, 2011.

Wang, G., Zhang, R., Gomez, M. E., Yang, L., Levy Zamora, M., Hu, M., Lin, Y., Peng, J., Guo, S., Meng, J., Li, J., Cheng, C., Hu, T., Ren, Y., Wang, Y., Gao, J., Cao, J., An, Z., Zhou, W., Li, G., Wang, J., Tian, P., Marrero-Ortiz, W., Secrest, J., Du, Z., Zheng, J., Shang, D., Zeng, L., Shao, M., Wang, W., Huang, Y., Wang, Y., Zhu, Y., Li, Y., Hu, J., Pan, B., Cai, L., Cheng, Y., Ji, Y., Zhang, F., Rosenfeld, D., Liss, P. S., Duce, R. A., Kolb, C. E., and Molina, M. J.: Persistent sulfate formation from London Fog to Chinese haze, Proc. Natl. Acad. Sci. U. S. A., 113, 13630-13635, 10.1073/pnas.1616540113, 2016.

Wang, Y., Jin, X., Liu, Z., Wang, G., Tang, G., Lu, K., Hu, B., Wang, S., Li, G., An, X., Wang, C., Hu, Q., He, L., Zhang, F., and Zhang, Y.: Progress in quantitative research on the relationship between atmospheric oxidation and air quality, J. Environ. Sci., 123, 350-366, 10.1016/j.jes.2022.06.029, 2023.

Xu, J. L., Griffin, R. J., Liu, Y., Nakao, S., and Cocker, D. R.: Simulated impact of NOx on SOA formation from oxidation of toluene and m-xylene, Atmos. Environ., 101, 217-225, 10.1016/j.atmosenv.2014.11.008, 2015a.

Xu, L., Kollman, M. S., Song, C., Shilling, J. E., and Ng, N. L.: Effects of NOx on the volatility of secondary organic aerosol from isoprene photooxidation, Environ. Sci. Technol., 48, 2253-2262, 10.1021/es404842g, 2014.

Xu, L., Guo, H. Y., Boyd, C. M., Klein, M., Bougiatioti, A., Cerully, K. M., Hite, J. R., Isaacman-VanWertz, G., Kreisberg, N. M., Knote, C., Olson, K., Koss, A., Goldstein, A. H., Hering, S. V., de Gouw, J., Baumann, K., Lee, S. H., Nenes, A., Weber, R. J., and Ng, N. L.: Effects of anthropogenic emissions on aerosol formation from isoprene and monoterpenes in the southeastern United States, Proc. Natl. Acad. Sci. U. S. A., 112, 37-42, 10.1073/pnas.1417609112, 2015b.

Xu, Z. N., Nie, W., Liu, Y. L., Sun, P., Huang, D. D., Yan, C., Krechmer, J., Ye, P. L., Xu, Z., Qi, X. M., Zhu, C. J., Li, Y. Y., Wang, T. Y., Wang, L., Huang, X., Tang, R. Z., Guo, S., Xiu, G. L., Fu, Q. Y., Worsnop, D., Chi, X. G., and Ding, A. J.: Multifunctional products of isoprene oxidation in polluted atmosphere and their contribution to SOA, Geophys. Res. Lett., 48, ARTN e2020GL089276, 10.1029/2020GL089276, 2021.

Yu, S. S., Jia, L., Xu, Y. F., and Pan, Y. P.: Molecular composition of secondary organic aerosol from styrene under different NOx and humidity conditions, Atmos Res, 266, ARTN 105950, 10.1016/j.atmosres.2021.105950, 2022.

Zhang, H., Yee, L. D., Lee, B. H., Curtis, M. P., Worton, D. R., Isaacman-VanWertz, G., Offenberg, J. H., Lewandowski, M., Kleindienst, T. E., Beaver, M. R., Holder, A. L., Lonneman, W. A., Docherty, K. S., Jaoui, M., Pye, H. O. T., Hu, W., Day, D. A., Campuzano-Jost, P., Jimenez, J. L., Guo, H., Weber, R. J., de Gouw, J., Koss, A. R., Edgerton, E. S., Brune, W., Mohr, C., Lopez-Hilfiker, F. D., Lutz, A., Kreisberg, N. M., Spielman, S. R., Hering, S. V., Wilson, K. R., Thornton, J. A., and Goldstein, A. H.: Monoterpenes are the largest source of summertime organic aerosol in the southeastern United States, Proc. Natl. Acad. Sci. U. S. A., 115, 2038-2043, 10.1073/pnas.1717513115, 2018.

Zhao, D., Schmitt, S. H., Wang, M., Acir, I. H., Tillmann, R., Tan, Z., Novelli, A., Fuchs, H., Pullinen, I., Wegener, R., Rohrer, F., Wildt, J., Kiendler-Scharr, A., Wahner, A., and Mentel, T. F.: Effects of NOx and SO_2 on the secondary organic aerosol formation from photooxidation of α-pinene and limonene, Atmos. Chem. Phys., 18, 1611-1628, 10.5194/acp-18-1611-2018, 2018.